COBEM 2021 26th International Congress of Mechanical Engineering
ABCM Associação Brasileira de Engenharia e Ciências Mecânicas
November 22-26, 2021, Virtual Congress, Brazil

COB-2021-0407
EFFECT OF THE INCLINATION ANGLE ON THE HEAT TRANSFER OF A VISCOPLASTIC FLUID FLOWING THROUGH A PLANAR EXPANSION-CONTRACTION

Marcos Vinicius Teixeira Maciel
Luiz Paulo Borges Miranda
Daniel Dall'Onder dos Santos
Federal University of Uberlândia, João Naves de Ávila Av., 2121, Uberlândia, MG, 38.408-100, Brazil
marcos.aero@ufu.br, luiz.miranda@ufu.br, dallonder@ufu.br

Flavia Schwarz Franceschini Zinani
Mechanical Engineering Graduate Program, UNISINOS, Unisinos Av., 950, São Leopoldo, RS, 93.022-750, Brazil
fzinani@ufu.br

Abstract. *It is known that non-Newtonian fluids comprise a wide range of applications in several industrial sectors. In this way, the study of non-Newtonian fluids has a great horizon yet to be explored. In the present work, a yield stress flow is analyzed, motivated by its industrial interest, in particular at the food industry that processes and transports its products with the aid of pipelines. A numerical model was used to solve a viscoplastic flow inside a planar channel with an expansion followed by contraction. To model the viscoplastic behavior, the SMD function was chosen. This model has interesting properties for its application on numerical methods and all its parameters are rheological parameters. The OpenFOAM software was selected to perform all the simulations once it is one of the best open-source software for computational flow dynamics, and its characteristics are particularly fitted for non-Newtonian simulations. Five dimensionless parameters were used to define the flow: the Prandtl number, the Reynolds number, the plastic number, the Richardson number, and the Jump number. The cavity walls and the fluid at the inlet are kept at different temperatures, and the channel walls are considered insulated. The mixed convection effect is analyzed for the different geometry orientations in terms of the average Nusselt number, and the displacement efficiency (the ratio between the portion of the cavity with the shear stress higher than the yield stress and the total area of the cavity).*

Keywords: *mixed convection, planar channel, yield stress fluid, SMD model.*

1. INTRODUCTION

Processes involving non-Newtonian fluids are becoming increasingly common in diverse industrial sectors. Hence, there is an increasing necessity for experimental and numerical studies to better understand the flow and heat transfer in processes involving this class of fluids. In an early experimental work from the beginning of the '80s, Joshi and Bergles (1980) highlighted that further work in the area would be desirable to more accurately account for the substantial increases in heat transfer coefficients above Newtonian, constant property values. However, experiments involving complex non-Newtonian fluids, especially in an industrial context, could be highly costly and time-consuming (Owens and Phillips, 2002).

Via numerical simulations, Nouar *et al.* (1995) obtained correlations for the local Nusselt number and pressure drop considering the rheological properties of Herschel-Bulkley fluids and their temperature dependence for a cylindrical duct. Constant wall temperature and constant wall flux conditions were simulated. For the former case, the authors found that the velocity profile tends to a flat one. For the latter case, the velocity profile initially tends to a flat one, but due to the temperature effects, the velocity profile begins to tend to a developed profile. A similar study was performed by Soares *et al.* (1999). Hammad (2000) numerically investigated the flow of Bingham fluids through a sudden pipe expansion with a center-body placed upstream the expansion plane. The expansion blockage ratio, the non-dimensional yield stress, Reynolds, Prandtl, and Brinkman numbers effects were investigated. The author found three different flow patterns downstream of the expansion obtained with specific combinations of yield and Reynolds numbers. These flow patterns highly affect the local heat transfer rate. The author performed a related investigation in a non-obstructed expanding channel in a more recent work (Hammad, 2017). The thermal processing of power-law fluids in annular ducts concerning the power-law index, duct eccentricity, and thermal boundary conditions effects was numerically investigated by Manglik and Fang (2002). The eccentricity causes a non-uniform velocity distribution, leading to different behaviors in the narrow

and wide gaps when the fluid is shear thinning or shear thickening. Regarding the heat transfer, the overall trend is to have a lower peak of midplane temperatures when the fluid is pseudoplastic, and a much higher peak temperature when the fluid is dilatant. The Nusselt numbers for flows in concentric annular ducts decrease as the power-law index is increased, but eccentric ducts present an opposite trend. However, for Herschel-Bulkley fluids flowing under similar conditions, Soares *et al.* (2003) found that the Nusselt number is rather insensitive to the rheological behavior of the fluid.

The work of Miranda *et al.* (2021) presents a study of the effect of Reynolds number, the plastic number, and the flow intensity over some parameters as exchanged heat, displacement efficiency, and pressure loss in a viscoplastic flow inside a planar channel with an abrupt expansion followed by an abrupt contraction. The channel walls are kept insulated while cavity walls are kept at a constant temperature, creating a temperature gradient between the flow inlet and the cavity walls. The authors did not consider the buoyancy effects, so only half of the channel was simulated. It was identified that some combinations of the dimensionless parameters led to the formation of an active recirculation zone inside the cavity, and this flow pattern had a major influence over the heat exchange and the displacement efficiency.

Some works found in the literature focus their attention on the investigation of free convection heat transfer in viscoplastic fluids. Sairamu *et al.* (2013) performed numerical simulations of Bingham fluids heat transfer from a heated horizontal circular cylinder in a square cavity using the COMSOL solver, ranging the flow dimensionless parameters and the ratio between the cylinder diameter and the size of the square cavity. As the size of the cavity increases in relation to to the cylinder diameter, both Bingham and average Nusselt numbers increase. Free convection from a heated circular cylinder in Bingham fluid flows was investigated by Nirmalkar *et al.* (2014) ranging the Rayleigh, Prandtl, and Bingham numbers. The authors observed an increment in the unyielded regions as the Bingham number is progressively increased or when the Rayleigh number is decreased as the buoyancy-induced flow weakens. The overall heat transfer rate is highly linked to gradients on the surface of the heated cylinder.

Coupling the two convection heat transfer mechanisms, Bose *et al.* (2015) and Nalluri *et al.* (2015) simulated the mixed heat transfer in Bingham fluids for a heated cylinder and a heated hemisphere, respectively. Both studies observed that increasing Reynolds or Prandtl numbers tend to enhance convection and the size of the yielded regions have a positive dependence on these parameters. On the other hand, the Bingham and Richardson numbers tend to stabilize the flow by suppressing the propensity of flow detachment from the surface of the cylinder. The average Nusselt number and drag coefficient show a positive dependence on the Richardson number, but this dependence progressively weakens with the increasing Bingham number. Srinivas *et al.* (2009) numerically studied the mixed convection heat transfer from a cylinder in power-law fluids and found that both drag coefficient and average Nusselt number are enlarged with the increasing buoyancy effects, Reynolds and Prandtl numbers. The decrease of the power-law index intensifies the drag and the heat transfer, whereas both of these parameters are generally reduced in shear-thickening fluids. The buoyancy effects were found to be stronger in shear-thinning fluids and at low Reynolds number regimes. Santos (2016) simulated the mixed convection from a cylinder immersed in viscoplastic fluids with a constant wall temperature. The drag coefficient and Nusselt number were obtained for different conditions ranging the power-law index, the Herschel-Bulkley number, and the Richardson number. The latter has a positive effect on the cylinder heat transfer and drag coefficient. The HB number presented two distinctive behaviors regarding the heat transfer: for HB < 500, the Nusselt number is increased due to a local increase of the velocity field close to the cylinder surface; for HB > 500, the viscoplastic effects become so strong that this local acceleration disappears. On the other hand, the increase of the power-law index decreases the heat transfer. The drag coefficient has a significant increment with the increase of both HB number and n index.

The geometry inclination influence has been recently investigated for 2-D planar branching channel flows for power-law and Bingham fluids by Maurya *et al.* (2019) and Maurya *et al.* (2021), respectively, and for a heated cone in Bingham fluids by Mishra *et al.* (2018). However, the buoyancy effects were not taken into account. In a more realistic setting, especially when the Richardson number does not tend to 0 (or even can be around 1), mixed convection must be considered in numerical simulations. In this situation, the geometry inclination has major effects on the walls' local Nusselt number profiles and the overall heat transfer. Thus, this work aims to numerically investigate the laminar mixed convection of an SMD viscoplastic fluid on a planar expansion followed by a contraction taking into account the geometry inclination. All fluid and flow properties are kept constant, and the geometry is rotated from -90° to 90° regarding the horizontal position. The influence of the geometry inclination is evaluated on the average Nusselt number at the upper and bottom walls, as well as on the unyielded regions morphology.

2. MECHANICAL MODEL

The mechanical model employed in this work to describe non-isothermal and incompressible flows of viscoplastic fluids was formed by coupling the mass, momentum and energy balance equations with the modified SMD model (de Souza Mendes and Dutra (2004) and de Souza Mendes (2009)):

$$\eta(\dot{\gamma}) = \left(1 - exp\left(-\frac{\eta_0}{\tau_0}\dot{\gamma}\right)\right)\left(\frac{\tau_0}{\dot{\gamma}} + K\dot{\gamma}^{n-1}\right) + \eta_\infty \tag{1}$$

where τ_0 is the yield stress limit of the material, K is the consistency index, η_0 and η_∞ are, respectively, the viscosities for very low and high values of the shear rate; n is the power-law index, which controls the shear-thinning (and eventually the shear-thickening) of the viscosity when the material starts to flow. The SMD model has a qualitative behavior observed for most viscoplastic liquids of interest: a high-viscosity plateau at low shear rates, followed by a sharp drop of the viscosity level leading to a power-law region and a low-viscosity plateau for higher shear rate values – this last part is added to avoid a zero viscosity non-physical behavior. The coupled velocity, stress, and temperature fields are governed by the following equations:

$$\begin{aligned} &\text{div } \mathbf{u} = 0 \\ &\rho(\nabla \mathbf{u})\mathbf{u} = -\nabla p + \text{div } \boldsymbol{\tau} + \rho \mathbf{g}\beta(T - T_{ref}) \\ &\boldsymbol{\tau} = 2\eta(\dot{\gamma})\mathbf{D}(\mathbf{u}) \\ &\rho c_p(\nabla T)\mathbf{u} = \kappa \nabla^2 T \end{aligned} \tag{2}$$

where $\mathbf{u}$ is the velocity vector, p the hydrostatic pressure, $\mathbf{D}$ the strain rate tensor, $\boldsymbol{\tau}$ is the extra-stress tensor, β is the volumetric thermal expansion coefficient, T the temperature, and T_{ref} a reference temperature, $\mathbf{g}$ the gravity vector; ρ, c_p, and κ are, respectively, the fluid density, specific heat, and thermal conductivity; η is the non-Newtonian viscosity, function of the shear-rate-dependent defined as $\dot{\gamma} = (2tr\mathbf{D}^2)^{1/2}$.

2.1 Dimensionless groups of interest

In this work, the dimensionless groups of interest are: the Reynolds number, the Prandtl number, the jump number, the plastic number, the Richardson number, and the Nusselt number. The expressions for the Reynolds number (*Re*), the Prandtl number (*Pr*) and plastic number (*Pl*) adopted are the definitions proposed by Thompson and Soares (2016), as follows:

$$Re = \frac{\rho {U_c}^2}{\tau_0 + K(\frac{U_c}{L_c})^n + \eta_\infty(\frac{U_c}{L_c})} \tag{3}$$

$$\frac{1}{Pr} = \frac{K(\frac{U_c}{L_c})^n + \eta_\infty(\frac{U_c}{L_c})}{\tau_0 + K(\frac{U_c}{L_c})^n + \eta_\infty(\frac{U_c}{L_c})} \frac{\rho\alpha}{K(\frac{U_c}{L_c})^{n-1} + \eta_\infty} \tag{4}$$

$$Pl = \frac{\tau_0}{\tau_0 + K(\frac{U_c}{L_c})^n + \eta_\infty(\frac{U_c}{L_c})} \tag{5}$$

where α is the thermal diffusivity, U_c and L_c are the characteristic velocity and the characteristic length, respectively taken as the value of the velocity at the inlet and the half channel height (H_1).

The jump number (*J*) is an dimensionless group proposed by de Souza Mendes *et al.* (2007), and its expression is:

$$J = \frac{\eta_0 \dot{\gamma}_1}{\tau_0} - 1 \tag{6}$$

where $\dot{\gamma}_1 = \left(\frac{\tau_0}{K}\right)^{\frac{1}{n}}$.

The dimensionless apparent viscosity for high shear rates and the Richardson number are defined as:

$$\eta^*_\infty = \frac{\eta_\infty \dot{\gamma}_1}{\tau_0} \tag{7}$$

$$Ri = \frac{|\mathbf{g}|\beta(T_s - T_{ref})L_c}{U_c^2} \tag{8}$$

The displacement efficiency Φ_{de} can be defined as:

$$\Phi_{de} = 1 - \frac{A_{cav,0}}{A_{cav}} \tag{9}$$

where Δp_c is the pressure difference from two different positions where the flow is fully developed (one upstream in the channel and the other downstream in the channel). Δp_s is the difference in pressure obtained in a simple channel at the same points used to obtain Δp_c, and its value is obtained via a numerical method used to solve the balance equations with

fully developed flow conditions. hlTo calculate Δp_c, only the horizontal channel was considered. $A_{cav,0}$ is the area of the apparent unyielded zones inside the cavity, and A_{cav} is the total surface of the cavity.

The dimensionless position vector ($\mathbf{x}^*$), dimensionless velocity ($\mathbf{u}^*$), dimensionless pressure (p^*), dimensionless strain rate ($\dot{\gamma}^*$), dimensionless shear rate (τ^*), dimensionless apparent viscosity (η^*), and dimensionless temperature (T^*) are defined as:

$$\mathbf{x}^* = \frac{\mathbf{x}}{L_c} \qquad \mathbf{u}^* = \frac{\mathbf{u}}{\dot{\gamma}_1 L_c} \qquad p^* = \frac{p}{\tau_0} \qquad \dot{\gamma}^* = \frac{\dot{\gamma}}{\dot{\gamma}_1} \qquad \tau^* = \frac{\tau}{\tau_0} \qquad \eta^* = \frac{\eta\dot{\gamma}_1}{\tau_0} \qquad T^* = \frac{T - T_{ref}}{T_{wall} - T_{ref}} \tag{10}$$

The average Nusselt ($\bar{Nu}$) was calculated as described by Miranda *et al.* (2021).

2.2 Geometry and boundary conditions

The flow along a planar channel containing a sudden expansion followed by a sudden contraction (henceforward referred as a cavity) is numerically investigated, and the geometry dimensions are shown in Fig. 1. The ratio between dimension H_2 (half cavity height) and dimension H_1 (half channel height) is equal to 6.3. The ratio of L_2 (length of the expanded region) to H_2 is equal to 1 and the ratio of L_1 (length of the channel) and H_1 is equal to 16.85. Thus, the analyzed domain has a total length of 40 units.

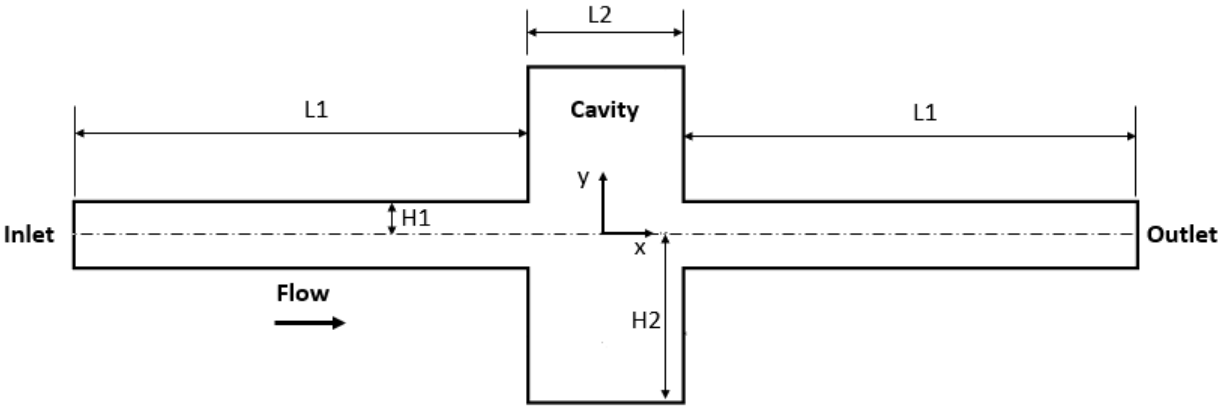

Figure 1. Geometry of the planar channel.

The velocity boundary conditions were impermeability and no-slip on the channel and cavity walls and a flat horizontal velocity profile at the inlet. The fluid enters the geometry with $T^* = 0$. The channel walls were considered thermally insulated whilst the temperature at cavity walls is kept constant ($T^* = 1$).

To evaluate the influence of geometry's angle of inclination (θ) on the heat transfer, a default set of dimensionless numbers was chosen to perform the numerical simulations. This default set is presented in Tab. 1, alongside the default set adopted by Miranda *et al.* (2021). Besides these differences in the default set, the geometry adopted by Miranda *et al.* (2021) has a symmetry line, while the present work simulated the whole planar channel due to the influence of the gravitational forces.

Table 1. Default dimensionless set adopted by the present work and by Miranda *et al.* (2021).

Parameter	Re	Pl	n	J	Pr	η^*_∞	Ri
Miranda *et al.* (2021)	25	0.4	0.5	10000	14	0.01	0
Present Work	25	0.4	0.5	1000	129	0	1

The free software OpenFoam was employed to solve the flow, and the numerical mesh adopted follows the same mesh pattern proposed by Miranda *et al.* (2021), being the only difference the absence of the symmetry line. Thus the adopted mesh in the present work has twice the number of elements when compared with Miranda *et al.* (2021) mesh.

3. RESULTS

To analyze the effect of the inclination angle over the flow and temperature fields, simulations were performed ranging it from -90° (the flow and the gravity vector are aligned and are on the same direction) to 90° (the flow and the gravity vector are aligned and are on opposite directions). The unyielded regions (black areas on Figs. 2c and 3) were obtained considering the areas where the shear rate is lower than the shear rate at which $\tau = \tau_0$.

3.1 Horizontal channel

In this first section, the horizontal channel is analyzed in more detail, allowing a deeper understanding of the general mechanisms involved in this flow. This configuration has a direct counterpart at Miranda *et al.* (2021), with only the aforementioned differences at the dimensionless parameters set. In the horizontal channel, the gravity is normal to the flow direction. Figure 2 shows the velocity and the temperature fields, and the unyielded regions and streamlines for this configuration.

An important portion of the upper cavity is filled with apparent unyielded zones, including the near-wall regions. These apparent unyielded zones have almost null velocity magnitude and have a high viscosity, indicating that conduction heat transfer is more relevant inside the upper cavity. Even though some streamlines are indicating a recirculation zone inside the upper cavity, these streamlines cross static apparent unyielded zones, indicating that these recirculation zones also have a near null velocity. On the other hand, the lower cavity has significantly fewer static apparent unyielded zones, and the streamlines indicate at least two active recirculation zones. These recirculation zones increase the convection heat transfer, creates some regions with a temperature plateau, and even allows the formation of some moving apparent unyielded zones. This difference between static and moving apparent unyielded zones is important not only because of the heat transfer but also because of the renewing rate of the flow inside the cavity. Comparing these results with the counterpart at Miranda *et al.* (2021), it is possible to identify the importance of considering the buoyancy effects: when the buoyancy effects are neglected, not only the lower and upper cavity has the same results, but it is possible to identify only one recirculation zone inside the cavity.

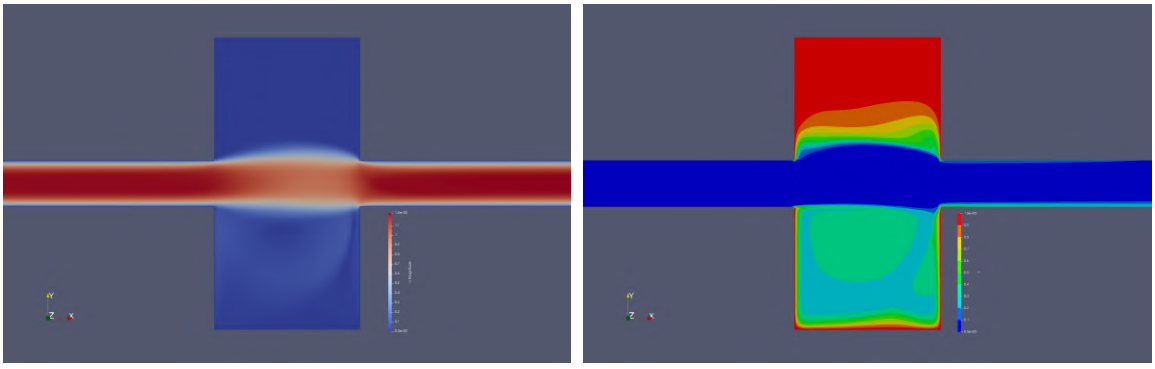

(a) $|U|$ (b) T

(c) Unyielded regions and streamlines

Figure 2. (a) Velocity magnitude; (b) temperature and (c) unyielded regions and streamlines of the horizontal channel.

3.2 Inclined channel

When buoyancy effects are considered, the flow has two driving forces: the inertia forces and the buoyancy forces. This is particularly remarkable when an inclined channel is considered, as the buoyancy forces are stronger where the temperature gradient is higher. In the adopted geometry, the temperature gradient is higher near the walls and corners of the cavity, and the buoyancy forces can significantly change the flow pattern inside these zones. Figure 3 shows the apparent unyielded zones and streamlines for channels with different inclination angles. Regarding the apparent unyielded zones, as a general rule, the more inclined the channel, there are less apparent unyielded zones, particularly static apparent unyielded zones. In a more inclined channel, the buoyancy forces component tangential to the horizontal wall is increased, strengthening the flow inside the cavity. For both θ=90° and θ=-90°, there are only moving apparent unyielded zones.

Figure 3 also shows a new flow pattern: when θ is negative, the buoyancy forces component tangential to the horizontal has the same orientation of the main flow, and thus the opposite direction of the recirculation zone. This way, the recirculation zone is gradually replaced by an extension of the main flow. This new flow pattern does not show a temperature plateau, as the recirculation zone does. Figure 4 shows the temperature fields for some channels with different inclination angles. On the other hand, when θ is positive, the recirculation zone is increased to the point where it gets bigger than the cavity itself, reducing the cross-section area of the main flow. Figure 5 shows the difference in the velocity field for θ=90° and θ=-90°.

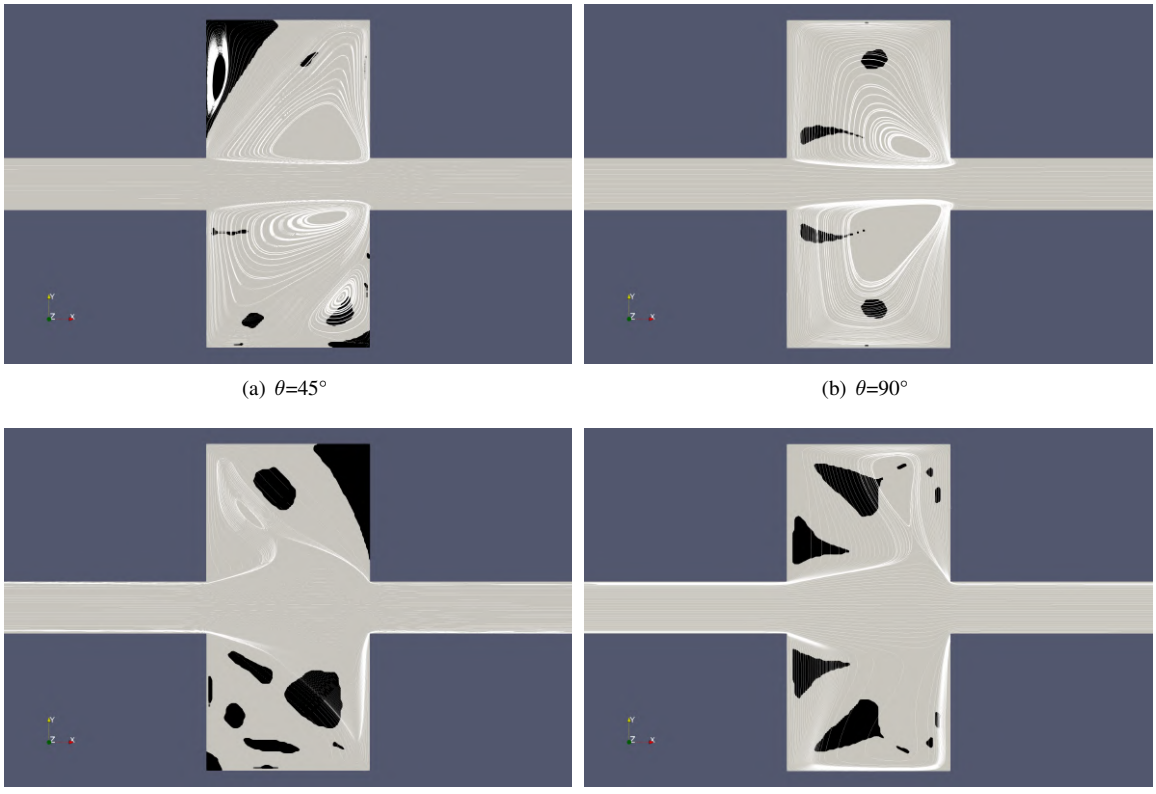

(a) θ=45° (b) θ=90°

(c) θ=-45° (d) θ=-90°

Figure 3. Apparent unyielded zones and streamlines for (a) θ=45°; (b) θ=90°; (c) θ=-45°; (d) θ=-90°.

3.3 Displacement efficiency

As already discussed, as a general trend, the more inclined the channel, the less apparent unyielded zones it has, no matter if θ is positive or negative. Figure 6 illustrates this trend in terms of displacement efficiency. The lowest displacement efficiency was measured at θ=0°, but near θ=-90° the value of the displacement efficiency decreases. This is due to the moving apparent unyielded zones that are formed inside the cavity, due to the flow pattern.

3.4 Average Nusselt number

The three flow patterns previously discussed have an important impact on heat exchange. The static apparent unyielded zones have the lower average Nusselt number because they rely on conductive heat exchange. Both the recirculation zone and the main flow extension increases the convective heat exchange, and Fig. 7 indicates that the main flow extension pattern is the most effective flow pattern in terms of heat exchange. Figure 7 does not show an abrupt change between these last two flow patterns, as they gradually replaced each other.

4. CONCLUSIONS

The present work discussed how the buoyancy forces affect the flow of a viscoplastic fluid inside a planar channel with an expansion-contraction cavity. The right choice of the inclination angle can increase the heat exchange inside the lower cavity by almost five times, without decreasing the heat exchange inside the upper cavity. The inclination angle can also prevent the formation of fouling layers of static apparent unyielded zones, assuring the renew rate of the flow.

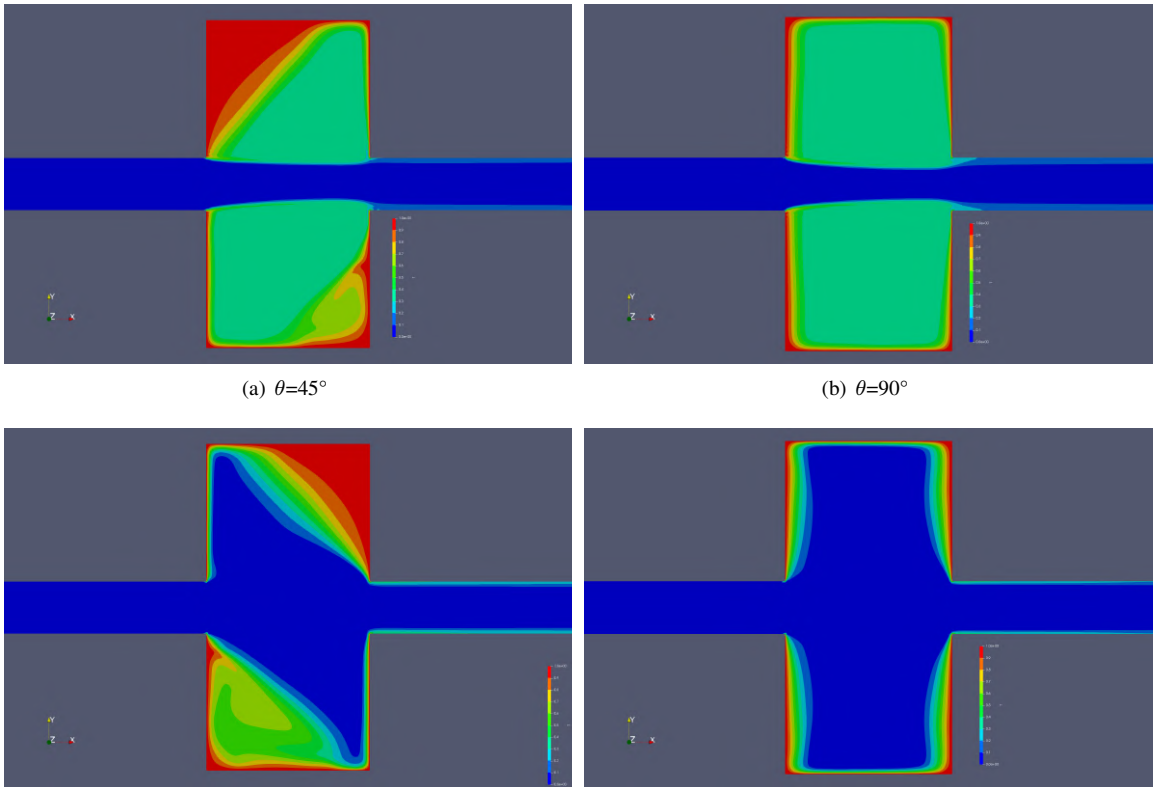

(a) θ=45° (b) θ=90°

(c) θ=-45° (d) θ=-90°

Figure 4. Temperature fields for (a) θ=45°; (b) θ=90°; (c) θ=-45°; (d) θ=-90°.

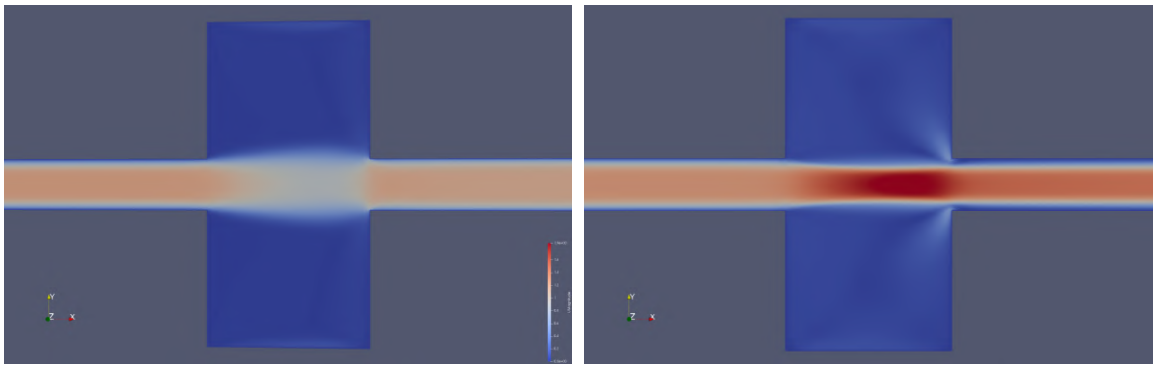

(a) θ=-90° (b) θ=90°

Figure 5. Velocity fields for (a) θ=-90°; (b) θ=90°, both figures share the same scale.

5. ACKNOWLEDGEMENTS

This study was financed in part by CAPES (Coordination for the Improvement of Higher Education Personnel) with finance Code 001. L. P.B. Miranda and F.S.F. Zinani are grant holders of CNPq, processes numbers 140729/2020-8 and 307827/2018-6, respectively. The authors also acknowledge FAMEPIG and the Faculty of Mechanical Engineering - UFU.

6. REFERENCES

Ahmadi, A. and Karimfazli, I., 2021. "A quantitative evaluation of viscosity regularization in predicting transient flows of viscoplastic fluids". *Journal of Non-Newtonian Fluid Mechanics*, Vol. 287, pp. 1–10.

Balmforth, N.J. and Rust, A.C., 2009. "Weakly nonlinear viscoplastic convection". *Journal of Non-Newtonian Fluid Mechanics*, Vol. 158, pp. 36–45.

Bose, A., Nirlmalkar, N. and Chhabra, R.P., 2015. "Effect of aiding-buoyancy on mixed-convection from a heated cylinder in Bingham plastic fluids". *Journal of Non-Newtonian Fluid Mechanics*, Vol. 220, pp. 3–21.

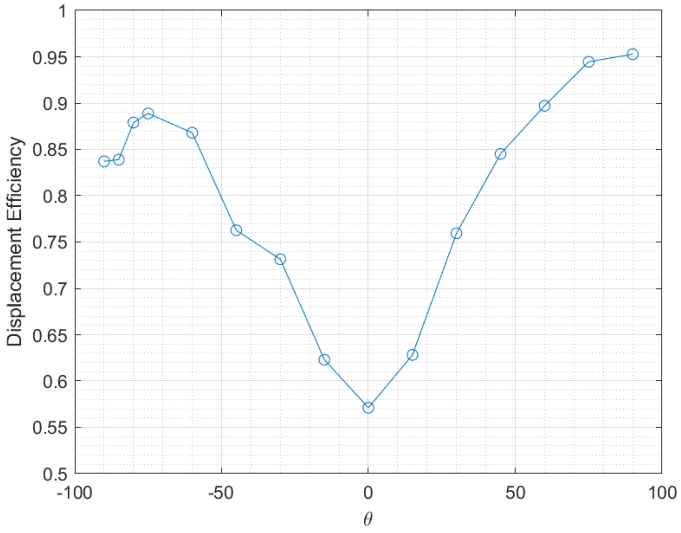

Figure 6. Displacement efficiency for -90°$\leq \theta \leq$ 90°.

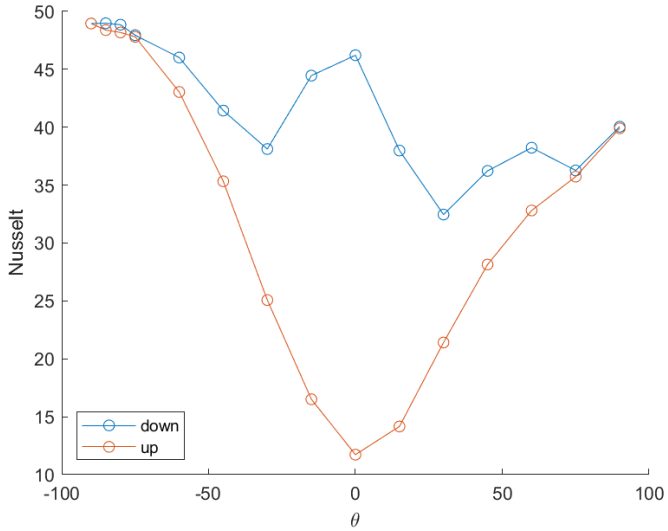

Figure 7. Average Nusselt number for the upper and lower cavities for -90°$\leq \theta \leq$ 90°.

De Los Reyes, J. and González-Andrade, S., 2013. "Numerical simulation of thermally convective viscoplastic fluids by semismooth second order type methods". *Journal of Non-Newtonian Fluid Mechanics*, Vol. 193, pp. 43–48.

de Souza Mendes, P.R., 2009. "Modeling the thixotropic behavior of structured fluids". *Journal of Non-Newtonian Fluid Mechanics*, Vol. 164, pp. 66–75.

de Souza Mendes, P.R. and Dutra, E.S.S., 2004. "Viscosity function for yield-stress liquids". *Applied Rheology*, Vol. 14, pp. 296–302.

de Souza Mendes, P.R., Naccache, M.F., Varges, P.R. and Marchesini, F.H., 2007. "Flow of viscoplastic liquids through axisymmetric expansions-contractions". *Journal of Non-Newtonian Fluid Mechanics*, Vol. 142, pp. 207–217.

Dutta, A., Gupta, A.K., Mishra, G. and Chhabra, R., 2018. "Effect of fluid yield stress and of angle of tilt on natural convection from a square bar in a square annulus". *Computers and Fluids*, Vol. 160, pp. 138–163.

Hammad, K.J., 2000. "The effect of hydrodynamic conditions on heat transfer in a complex viscoplastic flow field". *International Journal of Heat and Mass Transfer*, Vol. 43, No. 6, pp. 945–962. ISSN 0017-9310. doi:https://doi.org/10.1016/S0017-9310(99)00179-9. URL `https://www.sciencedirect.com/science/article/pii/S0017931099001799`.

Hammad, K.J., 2017. "Inertial thermal convection in a suddenly expanding viscoplastic flow field". *International Journal of Heat and Mass Transfer*, Vol. 106, pp. 829–840.

Hermany, L., Lorenzini, G., Klein, R., Zinani, F., dos Santos, E., Isoldi, L. and Rocha, L., 2018. "Constructal design applied to elliptic tubes in convective heat transfer cross-flow of viscoplastic fluids". *International Journal of Heat*

and Mass Transfer, Vol. 116, pp. 1054–1063.

Joshi, S. and Bergles, A., 1980. "Experimental study of laminar heat transfer to in-tube flow of non-Newtonian fluids". *Journal of JHeat Transfer*, Vol. 102, pp. 397–401.

Kefayati, G. and Tang, H., 2018. "MHD mixed convection of viscoplastic fluids in different aspect ratios of a lid-driven cavity using LBM". *International Journal of Heat and Mass Transfer*, Vol. 124, pp. 344–367.

Manglik, R. and Fang, P., 2002. "Thermal processing of viscous non-newtonian fluids in annular ducts: effects of power-law rheology, duct eccentricity, and thermal boundary conditions". *International Journal of Heat and Mass Transfer*, Vol. 45, No. 4, pp. 803–814. ISSN 0017-9310. doi:https://doi.org/10.1016/S0017-9310(01)00186-7. URL https://www.sciencedirect.com/science/article/pii/S0017931001001867.

Maurya, A., Tiwari, N. and Chhabra, R.P., 2019. "Effect of inclination angle on the forced convective flow of a power-law fluid in a 2-D planar branching channel". *International Journal of Heat and Mass Transfer*, Vol. 134, pp. 768–783.

Maurya, A., Tiwari, N. and Chhabra, R.P., 2021. "Forced convective flow of Bingham plastic fluids in a branching channel with the effect of T-channel branching angle". *Journal of Fluids Engineering*, Vol. 143, pp. 051201–1–051201–20.

Miranda, L.P.B., dos Santos, D.D. and Zinani, F.S.F., 2021. "Effects of reynolds number, plastic number, and flow intensity on the flow and on the heat transfer of a viscoplastic fluid flowing through a planar expansion followed by a contraction". *International Communications in Heat and Mass Transfer*, Vol. 120, p. 105038. ISSN 0735-1933. doi:https://doi.org/10.1016/j.icheatmasstransfer.2020.105038. URL https://www.sciencedirect.com/science/article/pii/S0735193320305650.

Mishra, P., Patel, S.A., Trivedi, M. and Chhabra, R.P., 2019. "Effect of power-law fluid behavior on Nusselt number of a circular disk in the forced convection regime". *Journal of Heat Transfer*, Vol. 141, pp. 041701–1–041701–8.

Mishra, P., Tiwari, A. and Chhabra, R.P., 2018. "Effect of orientation on forced convection heat transfer from a heated cone in Bingham plastic fluids". *International Communications in Heat and Mass Transfer*, Vol. 93, pp. 34–40.

Nalluri, S.V., Patel, S.A. and Chhabra, R., 2015. "Mixed convection from a hemisphere in Bingham plastic fluids". *International Journal of Heat and Mass Transfer*, Vol. 84, pp. 304–318.

Nascimento, U., Macêdo, E. and Quaresma, J., 2002. "Thermal entry region analysis through the finite integral transform technique in laminar flow of bingham fluids within concentric annular ducts". *International Journal of Heat and Mass Transfer*, Vol. 45, No. 4, pp. 923–929. ISSN 0017-9310. doi:https://doi.org/10.1016/S0017-9310(01)00187-9. URL https://www.sciencedirect.com/science/article/pii/S0017931001001879.

Nirmalkar, N., Bose, A. and Chhabra, R.P., 2014. "Free convection from a heated circular cylinder in Bingham plastic fluids". *International Journal of Thermal Sciences*, Vol. 83, pp. 33–44.

Nouar, C., Lebouché, M., Devienne, R. and Riou, C., 1995. "Numerical analysis of the thermal convection for herschel-bulkley fluids". *International Journal of Heat and Fluid Flow*, Vol. 16, No. 3, pp. 223–232. ISSN 0142-727X. doi:https://doi.org/10.1016/0142-727X(95)00010-N. URL https://www.sciencedirect.com/science/article/pii/0142727X9500010N.

Owens, R.G. and Phillips, T.N., 2002. *Computational Rheology*. Imperial College Press.

Patel, S.A. and Chhabra, R.P., 2019. "Buoyancy-assisted flow of yield stress fluids past a cylinder: Effect of shape and channel confinement". *Applied Mathematical Modelling*, Vol. 75, pp. 892–915.

Sairamu, M., Nirmalkar, N. and Chhabra, R., 2013. "Natural convection from a circular cylinder in confined Bingham plastic fluids". *International Journal of Heat and Mass Transfer*, Vol. 60, pp. 567–581.

Santos, D.D., 2016. "Numerical simulation of mixed convection from a cylinder immersed in viscoplastic fluids". In *Proceedings of the 16th Brazilian Congress of Thermal Sciences and Engineering - ENCIT 2016*. Vitória, Brazil.

Sasmal, C., Gupta, A. and Chhabra, R., 2019. "Natural convection heat transfer in a power-law fluid from a heated rotating cylinder in a square duct". *International Journal of Heat and Mass Transfer*, Vol. 129, pp. 975–996.

Soares, E.J., Naccache, M.F. and Souza Mendes, P.R., 2003. "Heat transfer to viscoplastic materials flowing axially through concentric annuli". *International Journal of Heat and Fluid Flow*, Vol. 24, No. 5, pp. 762–773. ISSN 0142-727X. doi:https://doi.org/10.1016/S0142-727X(03)00066-3. URL https://www.sciencedirect.com/science/article/pii/S0142727X03000663.

Soares, M., Naccache, M.F. and Souza Mendes, P.R., 1999. "Heat transfer to viscoplastic materials flowing laminarly in the entrance region of tubes". *International Journal of Heat and Fluid Flow*, Vol. 20, No. 1, pp. 60–67. ISSN 0142-727X. doi:https://doi.org/10.1016/S0142-727X(98)10044-9. URL https://www.sciencedirect.com/science/article/pii/S0142727X98100449.

Srinivas, A.T., Bharti, R.P. and Chhabra, R.P., 2009. "Mixed convection heat transfer from a cylinder in power-law fluids: effect of aiding buoyancy". *Industrial & Engineering Chemistry Research*, Vol. 48, pp. 9735–9754.

Thompson, R.L. and Soares, E.J., 2016. "Viscoplastic dimensionless numbers". *Journal of Non-Newtonian Fluid Mechanics*, Vol. 238, pp. 57–64.

7. RESPONSIBILITY NOTICE

The authors are solely responsible for the printed material included in this paper.